

Projectile breakup dynamics for ${}^6\text{Li} + {}^{59}\text{Co}$: kinematical analysis of α - d coincidences

F. A. Souza^{1a}, N. Carlin¹, C. Beck², N. Keeley³, A. Diaz-Torres⁴, R. Liguori Neto¹, C. Siqueira-Mello¹, M. M. de Moura¹, M. G. Munhoz¹, R. A. N. Oliveira¹, M. G. Del Santo¹, A. A. P. Suaide¹, E. M. Szanto¹, and A. Szanto de Toledo¹

¹ Instituto de Física - Universidade de São Paulo, Departamento de Física Nuclear, C.P. 66318, 05315-970, São Paulo-SP, Brazil

² Institut Pluridisciplinaire Hubert Curien, UMR 7178, CNRS-IN2P3 et Université Louis Pasteur, Boîte Postale 28, F-67037 Strasbourg, Cedex 2, France

³ Department of Nuclear Reactions, The Andrzej Sołtan Institute for Nuclear Studies, ul. Hoża 69, 00-681 Warsaw, Poland.

⁴ Department of Physics, Faculty of Engineering and Physical Sciences, University of Surrey, Guildford, GU2 7XH, UK

Received: date / Revised version: date

Abstract. A study of the kinematics of the α - d coincidences in the ${}^6\text{Li} + {}^{59}\text{Co}$ system at a bombarding energy of $E_{lab} = 29.6$ MeV is presented. With exclusive measurements performed over different angular intervals it is possible to identify the respective contributions of the sequential projectile breakup and direct projectile breakup components. A careful analysis using a semiclassical approach of these processes provides information on both their lifetime and their distance of occurrence with respect to the target. Breakup to the low-lying (near-threshold) continuum is delayed, and happens at large internuclear distances. This suggests that the influence of the projectile breakup on the complete fusion process can be related essentially to direct breakup to the ${}^6\text{Li}$ high-lying continuum spectrum.

PACS. 25.70.Mn Projectile and target fragmentation

1 Introduction

The breakup process in reactions induced by weakly bound nuclei (such as ${}^6\text{Li}$, ${}^7\text{Li}$, and/or ${}^9\text{Be}$) and its influence on

^a e-mail: fsouza@dfn.if.usp.br

the fusion cross section has been the subject of several experimental and theoretical investigations in the recent period [1,2,3,4,5,6,7,8,9,10,11,12,13,14,15,16,17,18,19,20]. In inclusive experiments, the light particle spectra measured in ‘singles’ mode display significant contributions from reaction mechanisms other than projectile breakup. This was for example shown very recently for the well studied ${}^6\text{Li} + {}^{59}\text{Co}$ system [20]. Therefore, coincidence measurements are of crucial importance to disentangling the respective contributions of the non-capture projectile breakup components (both direct and sequential) from other competing mechanisms such as incomplete fusion (ICF) and/or transfer (TR). In this context, great effort has to be made in the possible distinction between ICF and TR (see for instance ref. [21]). In particular, the consideration of either total fusion cross sections or complete fusion (CF) cross sections has proved to be important for a better understanding of the competition between the different mechanisms and their respective influence on the fusion process. The contributions of sequential projectile breakup (SBU) and direct projectile breakup (DBU) are both significant and it is necessary to determine which process influences CF most. In this case, the study of the breakup dynamics could provide decisive information.

The direct breakup DBU seems to be the main cause of the above-barrier CF suppression in the ${}^9\text{Be} + {}^{208}\text{Pb}$ system, as shown in [22] through sub-barrier measurements of the breakup probability as a function of the distance of closest approach. This is a key ingredient for a novel classical trajectory model with stochastic breakup [23] which

quantitatively relates the breakup process to ICF and CF cross sections.

In this work, we present the results of α - d coincidence measurements (non-capture breakup events) for the ${}^6\text{Li} + {}^{59}\text{Co}$ system at a bombarding energy of $E_{lab} = 29.6$ MeV, about twice the energy of the Coulomb barrier. By using a simple 3-body kinematics analysis we demonstrate that the ICF/TR processes on the one hand, and the projectile breakup components (SBU and DBU) on the other, are associated with quite different angular intervals. We also present results for an investigation of the breakup dynamics, by means of calculations related to semiclassical considerations [24] involving barrier tunnelling, lifetimes and distances of closest approach for the Coulomb trajectories of the projectile and outgoing fragments.

2 Experimental Setup

The experiment was performed at the University of São Paulo Pelletron Laboratory, using the 8 UD Tandem accelerator. The 30 MeV ${}^6\text{Li}$ beam was provided by a SNICS ion source and bombarded a 2.2 mg/cm^2 ${}^{59}\text{Co}$ target. After correction for energy loss in the target, the effective bombarding energy is $E_{lab} = 29.6$ MeV ($E_{cm} = 26.9$ MeV) more than twice the energy ($E_{cm} \approx 12$ MeV) corresponding to the Coulomb barrier. The beam current on target was about 10 nA. We used 11 triple telescopes [25] for the detection and identification of the light particles, positioned on both sides with respect to the beam direction with 10° spacing, covering angular intervals from -45° to -15° and 15° to 75° . The telescopes consisted of an

ion chamber with a $150 \mu\text{g}/\text{cm}^2$ aluminized polypropylene entrance window, a $150 \mu\text{m}$ thick Si surface barrier detector and a CsI detector with PIN diode readout. The ion chamber was operated with 20 torr of isobutane.

Additional details of the experimental setup and light charged particle analysis can be found elsewhere [20,25].

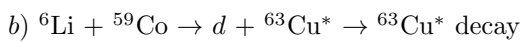
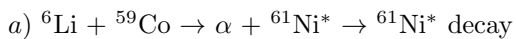
3 Results and discussion

In a previous publication [20], we investigated the kinematics of the inclusive α and d energy spectra. After subtraction of the estimated compound nucleus contributions, broad bumps with significant yields remained in both the α and d spectra. The behaviour of the energy centroids of these bumps as a function of the detection angle was found to be consistent with dominant contributions from incomplete fusion and/or transfer components i.e.:

α -incomplete fusion (α -ICF)/ α -transfer (α -TR) for the d spectra and,

d -incomplete fusion (d -ICF)/ d -transfer (d -TR) for the α spectra.

These processes are represented, respectively, as follows:



The corresponding excitation energies (associated with the energy centroids of the bumps) were 24.6 MeV and 22.5 MeV for the ${}^{61}\text{Ni}$ and ${}^{63}\text{Cu}$ nuclei, respectively.

In fig. 1 typical α - d coincidence two-dimensional spectra are displayed. For angular differences within the ${}^6\text{Li}$ breakup cone corresponding to the (2.186 MeV, 3^+) first resonant state, we observe two peaks from the two possible kinematical solutions of the SBU. We also observed a broad structure between the two sharp peaks. Alpha- d decay of the second excited state (3.562 MeV, 0^+) of ${}^6\text{Li}$ is forbidden due to parity considerations and no peak due to the third excited state (4.312 MeV, 2^+) was observed. No evidence of decays from higher-lying resonant states was seen. For angular differences larger than the SBU cone, we observed only broad structures. These broad structures could be associated either with the decay of nuclei produced in ICF/TR (incomplete fusion and/or transfer) or to ${}^6\text{Li}$ DBU to the continuum. It is interesting to note that these non-resonant contributions were assumed to arise exclusively from DBU in the case of the ${}^6\text{Li} + {}^{209}\text{Bi}$ reaction [19] at $E_{lab} = 36$ MeV and 40 MeV whereas ICF yields were found to represent a large fraction of the total reaction cross section in this energy range [10]. We cannot fully confirm this assumption as ICF/TR is not expected to have such a target dependence although ${}^{59}\text{Co}$ and ${}^{209}\text{Bi}$ nuclei belong to very different mass regions.

3.1 Kinematics of α - d coincidences

In order to identify the contributions of the different mechanisms included in the broad structures, we performed a 3-body kinematics [26] analysis of the α - d coincidence events. We present a study of the α and d energies as a function of angle and, as in previous work, we study

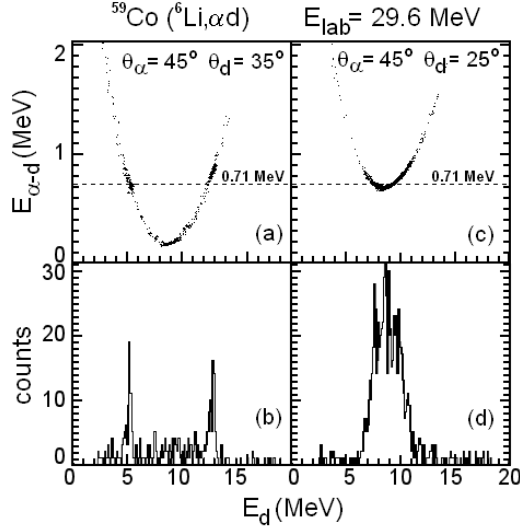


Fig. 1. a) The α - d relative energy $E_{\alpha d}$ as a function of the deuteron energy for $\theta_\alpha = 45^\circ$ and $\theta_d = 35^\circ$. b) The corresponding projection on the deuteron energy axis. c) and d) The same for $\theta_\alpha = 45^\circ$ and $\theta_d = 25^\circ$. The dashed lines correspond to 3-body kinematics calculations assuming α - d decays from the first resonant (2.186 MeV, 3^+) state of ${}^6\text{Li}$.

the behaviour of the energy centroids of the broad structures. For the case of fixed α -particle angle, if d -ICF/TR is dominant the α -particle energy should be constant, independent of the d emission angle. This energy should be consistent with the excitation energy of the intermediate ${}^{61}\text{Ni}$ nucleus. Similar behaviour would be expected for fixed d angle in the case of dominant α -ICF/TR; the d energy should be constant as a function of the α -particle emission angle and consistent with the excitation energy of the ${}^{63}\text{Cu}$ intermediate nucleus. On the other hand, as shown in [27,28], if ${}^6\text{Li}$ direct breakup is dominant, the centroid of the broad structure would approximately cor-

respond to the minimum allowed α - d relative energy for each angular pair (see fig. 1).

In fig. 2 we plot the d energy E_d as a function of θ_α for $\theta_d = 35^\circ$. In this case, if α -ICF/TR is dominant, the d energy E_d should be constant, consistent with the 22.5 MeV excitation energy of the ${}^{63}\text{Cu}$ intermediate nucleus (dotted line). This behaviour would be more evident for angles near the ${}^{63}\text{Cu}$ recoil direction, for which we expect the maximum of cross section for the α -particle decay. This is indeed observed for angles near the recoiling ${}^{63}\text{Cu}$. For other negative angles we observe instead a trend consistent with a 24.6 MeV excitation energy for the ${}^{61}\text{Ni}$ composite system (dot-dashed line). This suggests the dominance of the d -ICF/TR process. Therefore, both α -ICF/TR and d -ICF/TR contributions can be, in principle, mixed together. The behaviour of the minimum allowed α - d relative energy for ${}^6\text{Li}$ breakup is also shown in fig. 2 (dashed line). The observed trend suggests that the ${}^6\text{Li}$ DBU dominates in the case of angular pairs for which the broad structure is observed with $\Delta\theta_{\alpha d} = 10^\circ$ and 20° . For these angular pairs (i.e. for θ_α angle values ranging between 10° and 50°) the experimental points shown in fig. 2 correspond to the energies of the SBU peaks clearly visible in fig. 1(b) and extrapolated in fig. 1(d).

3.2 Breakup dynamics

In order to gain insight into the dynamics of the SBU and DBU processes, we use a semiclassical approximation, following the procedure previously adopted in [29]. This hypothesis is valid as long as the Sommerfeld parameter

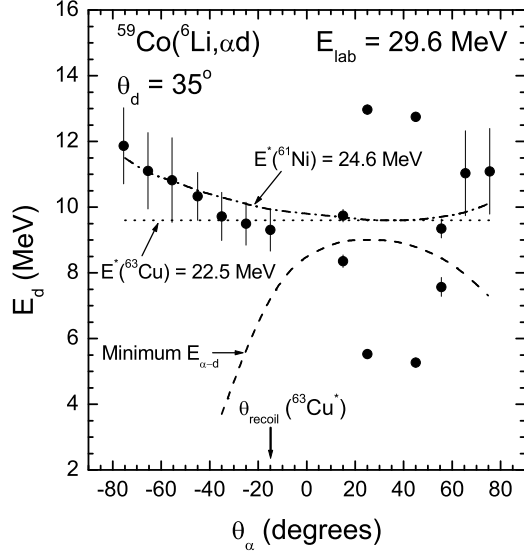


Fig. 2. Experimental values for the deuteron energy as a function of the α -particle detection angle. The 3-body kinematics predictions for ICF/TR and the minimum relative energy, $E_{\alpha d}$, for ${}^6\text{Li}$ breakup are also shown.

η is large ($\eta \sim 6$). High partial waves of the projectile-target relative motion dominate the non-capture breakup process, so the effect of the nuclear field on the projectile trajectory is very small. We can then assume that the projectile travels the target nuclear field following a Coulomb trajectory. This statement is also valid for the breakup fragments, as long as the relative energies are not too high.

The relation between the angle of emission and the distance of closest approach is:

$$R_{min} = \frac{Z_p Z_T e^2}{2E} \left[1 + \frac{1}{\sin(\theta/2)} \right] \quad (1)$$

where Z_p and Z_T are the projectile and target charge numbers, E is the centre-of-mass energy and θ is the scattering angle.

In order to obtain information on the distances of closest approach related to the occurrence of SBU and DBU, we define a quantity f which may be considered as the relative probability for the production of particles for a given process at a given distance of closest approach. The quantity f can be defined as follows:

$$f = \frac{1}{R_{min}} \frac{d\sigma}{dR_{min}} = -\frac{1}{R_{min}} \frac{16\pi E}{Z_p Z_T e^2} \sin(\theta/2) \frac{d\sigma}{d\Omega} \quad (2)$$

Here, $d\sigma/d\Omega$ is the differential cross section in the centre-of-mass rest frame for the process under consideration.

Figure 3 depicts the experimental angular distribution for the SBU process analyzed in ref. [20], as well as for the DBU. The angular distribution for the DBU is shown for ${}^6\text{Li}$ continuum excitation energies summed between $E^* = 1.66$ MeV and $E^* = 2.10$ MeV. In the semiclassical calculations, we adopted the most probable value of the excitation energy observed experimentally in this range, which is $E^* = 1.7$ MeV. The dotted line was extracted from ref. [20] and corresponds to the SBU CDCC calculation [17]. The dashed line represents the DBU CDCC result [17] for a ${}^6\text{Li}$ excitation energy range from $E^* = 1.48$ MeV (breakup threshold) to $E^* = 2.10$ MeV. The experimental DBU angular distribution and the corresponding CDCC result both present similar shapes although with slightly different magnitudes. This small difference can be attributed to the excitation energy range from $E^* = 1.48$ MeV to $E^* = 1.66$ MeV, considered in the CDCC calculations but not observed experimentally due to the angular separation of the detectors. In table 1 we present the experi-

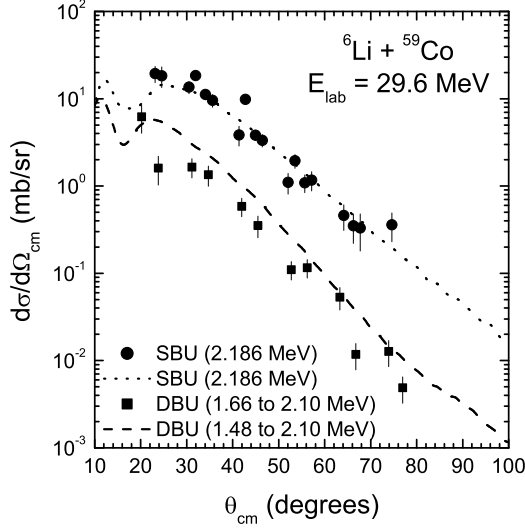


Fig. 3. Experimental angular distributions for the projectile sequential breakup (full circles) and direct breakup (full squares) processes, respectively. The dotted curve (CDCC calculation [17] for SBU) and dashed curve (CDCC calculation for DBU), as described in the text, are used for the semi-classical calculations of lifetimes and distance of occurrence discussed in fig. 4 and fig. 6.

Table 1. Experimental SBU and DBU cross sections and CDCC predictions.

	ΔE_{Exp}^* (MeV)	σ_{Exp} (mb)	ΔE_{CDCC}^* (MeV)	σ_{CDCC} (mb)
SBU [20]	2.186	20.6 ± 4.0	2.186	23.5
	1.66 - 2.10	3.04 ± 0.41	1.48 - 2.10	6.4
DBU	2.20 - 2.40	6.8 ± 4.2	2.20 - 2.40	2.7
	3.10 - 3.25	4.45 ± 0.94	2.41 - 3.98	11.9

mental ${}^6\text{Li}$ SBU cross section for the first resonant state (2.186 MeV, 3^+) [20] and experimental DBU cross sections for the three excitation energy intervals (ΔE^*) we observed, together with corresponding CDCC predictions for the sake of comparison.

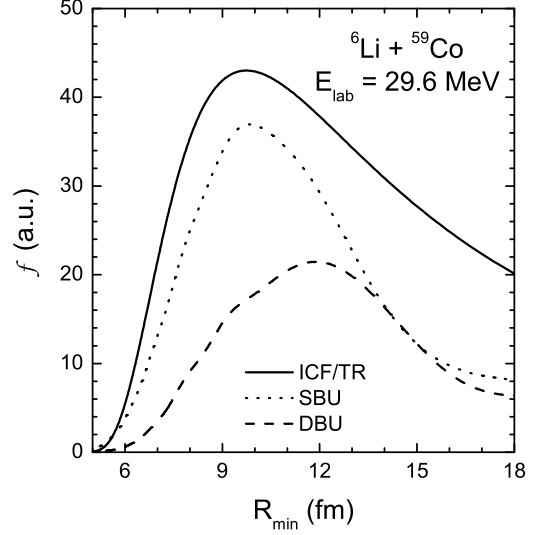


Fig. 4. Function f representing the relative probability for production of particles of a given process at a given distance of closest approach, as a function of R_{\min} for the projectile breakup processes SBU (dotted line) and DBU (dashed line), respectively.

The curves presented in fig. 3 were used for the calculation of the f functions shown in fig. 4 as a function of R_{\min} for the SBU and DBU processes. From the plots in fig. 4, one obtains the quantity R_{\min}^{MP} , the most probable value for R_{\min} for the process of interest.

In this work we also obtained insight into the lifetimes and distance of occurrence from the target for the SBU and DBU processes. In particular, for SBU we observed that the main contribution is due to the ${}^6\text{Li}$ 3^+ state with $E^* = 2.186$ MeV. For the DBU, the fragments are no longer bound by the nuclear potential, but are still under the influence of the Coulomb barrier between the α -particle and the d . This means that at least for the smaller relative energies, the DBU is a delayed process, as is the

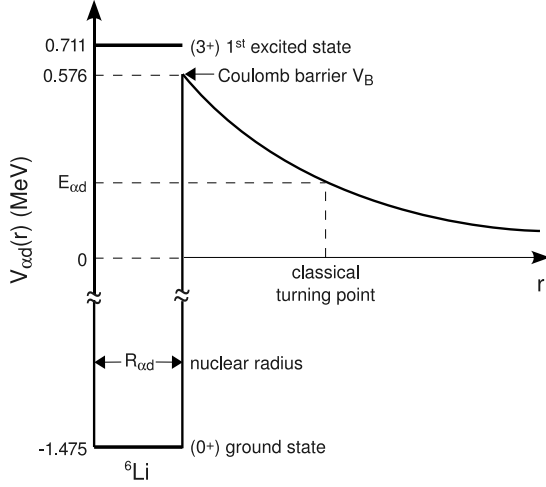


Fig. 5. Schematic representation of nuclear and Coulomb potentials as a function of the separation distance r between the α -particle and the d (adapted from ref. [24]).

SBU. A schematic representation of nuclear and Coulomb potentials is shown in fig. 5 (adapted from ref. [24]) as a function of the separation distance r between the α -particle and the d . The height of the Coulomb barrier $V_B = 0.576$ MeV was obtained using $R_{\alpha d} = 5.0$ fm and the breakup threshold is defined at $E_{\alpha d} = 0$.

In order to estimate the DBU lifetime due to barrier tunnelling, we adopt the model of [24], where it was assumed that, as in the theory of α decay, the decay rate of the unbound system can be written as:

$$\Lambda_l = \omega_l P_l \quad (3)$$

where ω_l is the barrier bouncing frequency, and P_l is the barrier transmission probability. Considering that we are dealing with relatively low α - d relative energies, only the s -wave case for which $l = 0$ will be considered, for simplicity. In this situation, the bouncing frequency can be estimated as being $\omega_0 = v_{\alpha d}/2R$, where $v_{\alpha d}$ is the α - d

relative velocity and R , the nuclear radius. The barrier transmission probability, according to the WKB approximation, is given by:

$$P_0 \approx \sqrt{\frac{V_B}{E_{\alpha d}}} \exp \left\{ -4\eta \left[\frac{\pi}{2} - \arcsin \sqrt{\frac{E_{\alpha d}}{V_B}} - \sqrt{\frac{E_{\alpha d}}{V_B} \left(1 - \frac{E_{\alpha d}}{V_B} \right)} \right] \right\} \quad (4)$$

where $\eta = Z_\alpha Z_d e^2 / \hbar v_{\alpha d}$ is the Sommerfeld parameter and $V_B = Z_\alpha Z_d e^2 / R_{\alpha d}$ is the height of Coulomb Barrier. The lifetime can then be determined as $\tau = 1/\Lambda$.

From first order perturbation theory, the differential cross section for Coulomb excitation is given by [30]:

$$\frac{d\sigma_{E\lambda}}{d\Omega} = \left(\frac{Z_T e}{\hbar v} \right)^2 a^{-2\lambda+2} B(E\lambda) \frac{df_{E\lambda}}{d\Omega}, \quad (5)$$

where a is half the distance of closest approach for a head-on collision, v is the initial relative velocity of projectile and target, $B(E\lambda)$ is the reduced transition probability and $df_{E\lambda}/d\Omega$ is the differential cross section function, which can be expressed as [24]:

$$\frac{df_{E\lambda}}{d\Omega} = \lim_{\tau \rightarrow \infty} h_{E\lambda}(\theta, \omega_C, \tau) \quad (6)$$

and

$$h_{E\lambda}(\theta, \omega_C, \tau) = \frac{(2\pi a^\lambda v)^2}{(2\lambda + 1)^3} \sin^{-4} \left(\frac{\theta}{2} \right) \sum_{\mu} \left| Y_{\lambda\mu} \left(\frac{\pi}{2}, 0 \right) \int_{-\tau}^{+\tau} \frac{(x + iy)^\mu}{r^{\lambda+\mu+1}} e^{i\omega t} dt \right|^2 \quad (7)$$

where ω_C is the frequency for Coulomb excitation, $Y_{\lambda\mu}$ are the spherical harmonics, (x, y) are Cartesian coordinates and r is the radial coordinate of the projectile in the focal system of the hyperbolic orbit. The function $h_{E\lambda}$ can be calculated in the time interval between $-\tau$ and $+\tau$ around $t = 0$, assumed to be the classical turning point. According

to the calculations shown in ref. [24], the time interval for Coulomb excitation is concentrated on ± 500 fm/c (1.67×10^{-21} s) around $t = 0$, independent of the multipolarity. The reference for measuring the lifetime is the time of the Coulomb excitation.

From the above considerations, one can estimate the distance between projectile and target when DBU occurs. According to [30,24], in the focal system of the hyperbolic orbit, the distance between projectile and target can be written as:

$$r = a[\varepsilon \cosh(s) + 1]. \quad (8)$$

Here, ε is the eccentricity parameter, given by $\varepsilon = 1/\sin(\theta^{MP}/2)$, with θ^{MP} being the scattering angle associated with R_{min}^{MP} . The parameter s [30,24] is related to the time t by:

$$t = \frac{a}{v}[\varepsilon \sinh(s) + s]. \quad (9)$$

As described above, from eq. 3 and $l = 0$, we can determine the lifetime $\tau_{DBU} = 1/\Lambda_{DBU}$ for the DBU states near threshold. In fig. 6 we present the plot of τ_{DBU} ($E_{lab} = 29.6$ MeV) as a function of $E_{\alpha d}$. Besides the ${}^6\text{Li}$ continuum at excitation energy $E^* = 1.7$ MeV shown in fig. 3, contributions from $E^* = 2.3$ MeV and 3.2 MeV were also observed. Using the ${}^6\text{Li}$ excitation energies and the corresponding values of τ_{DBU} , the values of r_{DBU} can be determined. The values of r_{DBU} can be compared to those obtained for SBU from the ${}^6\text{Li}$ 3^+ state with $E^* = 2.186$ MeV, and knowing that the SBU lifetime is $\tau_{SBU} = 2.73 \times 10^{-20}$ s, corresponding to $\Gamma_{SBU} = (0.024 \pm 0.002)$ MeV [31]. The results described above are summarized in table 2.

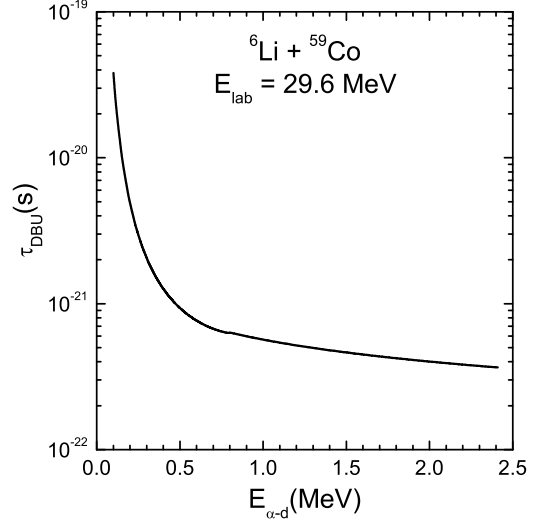


Fig. 6. Calculated lifetime of the DBU continuum states as a function of the relative energy $E_{\alpha d}$ from which the corresponding distances of occurrence can be deduced in table 2.

Table 2. Lifetimes, average distance of closest approach and distance of occurrence from the target for the projectile breakup components SBU and DBU.

	E^* (MeV)	τ (s)	R_{min}^{MP} (fm)	r (fm)
SBU	2.18	2.7×10^{-20}	8.5 ± 0.4	831.0 ± 1.3
	1.7	4.9×10^{-21}	9.2 ± 0.5	147.2 ± 1.7
DBU	2.3	6.3×10^{-22}	9.1 ± 0.7	19.8 ± 0.8
	3.2	4.4×10^{-22}	8.1 ± 1.2	14.3 ± 1.8

Table 2 shows that for all the processes we considered, the values of R_{min}^{MP} are very similar. However, the distances of occurrence are very distinct for the SBU and DBU. Due to the long lifetime of the resonant ${}^6\text{Li}$ first excited state, sequential projectile breakup occurs very far from the target. On the other hand, for DBU the shorter lifetimes of the continuum ‘states’ cause the breakup process to occur

at shorter distances from the target, although there are different distances for different excitation energies in the continuum.

The results obtained in this work are related to the non-capture breakup process. However, they can be extended to the case in which one of the fragments is captured by the target after projectile breakup. As observed in [20], from the investigation of the inclusive data, ICF/TR has been found to have the largest cross section, and therefore the major influence on the CF cross section. This conclusion appears to be also valid for a heavy target reaction such as ${}^6\text{Li} + {}^{209}\text{Bi}$ [19]. One may conclude from the results of the present work as well as from ref. [19] that the flux diverted from CF to ICF/TR would arise essentially from the DBU components (higher excitation energies in the continuum), as the SBU process or the low-lying DBU occur at large internuclear distances.

4 Summary

We investigated the kinematics for α - d coincidences registered for the ${}^6\text{Li} + {}^{59}\text{Co}$ reaction at $E_{\text{lab}} = 29.6$ MeV, approximately twice the energy of the Coulomb barrier. The analysis of the present exclusive data along with 3-body kinematics calculations allowed us to observe that the ICF/TR and the SBU/DBU processes are associated with different angular regions. A semiclassical approach, known to be valid for this low bombarding energy, was used to estimate the lifetime and distance of occurrence with respect to the target for these processes. The results indicate that projectile breakup to the low-lying (near-

threshold) continuum is delayed, and occurs at large internuclear distances. To conclude, for ${}^6\text{Li} + {}^{59}\text{Co}$ the influence of breakup on the CF process is essentially due to DBU to the ${}^6\text{Li}$ high-lying continuum spectrum.

The authors thank FAPESP and CNPq for financial support.

References

1. L. F. Canto, P. R. S. Gomes, R. Donangelo and M. S. Hussein, *Phys. Rep.* **424**, 1 (2006).
2. N. Keeley, R. Raabe, N. Alamanos, and J. L. Sida, *Prog. Part. Nucl. Phys.* **59**, 579 (2007); arXiv:**nucl-th:0702038**(2007) and references therein.
3. L. F. Canto, P. R. S. Gomes, J. Lubian, L. C. Chamon, E. Crema, *Nucl. Phys. A* **821**, 51 (2009).
4. M. Dasgupta *et al.*, *Phys. Rev. Lett.* **82**, 1395 (1999); arXiv:**nucl-ex/9901003**(1999).
5. V. Tripathi *et al.*, *Phys. Rev. Lett.* **88**, 172701 (2002).
6. C. Signorini *et al.*, *Phys. Rev. C* **67**, 044607 (2003).
7. C. Beck *et al.*, *Phys. Rev. C* **67**, 054602 (2003).
8. A. Diaz-Torres and I. J. Thompson, and C. Beck, *Phys. Rev. C* **68**, 044607 (2003); arXiv:**nucl-th/0307021**(2003).
9. A. Diaz-Torres, I. J. Thompson, *Phys. Rev. C* **65**, 024606 (2002); arXiv: **nucl-th/0111051**(2001).
10. M. Dasgupta *et al.*, *Phys. Rev. C* **70**, 024606 (2004).
11. P. R. S. Gomes *et al.*, *Phys. Rev. C* **71**, 017601 (2005);
12. G. V. Marti *et al.*, *Phys. Rev. C* **71**, 027602 (2005).
13. A. Shrivastava *et al.*, *Phys. Lett. B* **633**, 463 (2006).
14. A. Pakou *et al.*, *Phys. Lett. B* **633**, 691 (2006).
15. P. R. S. Gomes *et al.*, *Phys. Lett. B* **634**, 356 (2006).

16. C. Beck, A. S  nchez i Zafra, A. Diaz-Torres, I. J. Thompson, N. Keeley, and F. A. Souza, AIP Conferences Proceedings **853**, 384 (2006); Proc. of Fusion06 Conference, San Servolo, Venezia, Italy, 19-23 March 2006; arXiv:**nucl-th/0605029v2**(2006).
17. C. Beck, N. Keeley and A. Diaz-Torres, Phys. Rev. C **75**, 054605 (2007); arXiv:**nucl-th/0703085** (2007).
18. C. Beck, Nucl. Phys. A **787**, 251 (2007); arXiv:**nucl-ex/0701073** (2007); arXiv:**nucl-th/0610004** (2006).
19. S. Santra *et al.*, Phys. Lett. B **677**, 139 (2009).
20. F. A. Souza *et al.*, Nucl. Phys. A **821**, 36 (2009);arXiv:**0811.4556**(2009).
21. V. Tripathi *et al.*, Phys. Rev. C **72**, 017601 (2005).
22. D.J. Hinde, M. Dasgupta, B. R. Fulton, C. R. Morton, R. J. Wooliscroft, A. C. Berriman, and K. Hagino, Phys. Rev. Lett. **87**, 272701 (2002).
23. A. Diaz-Torres, D. J. Hinde, J. A. Tostevin, M. Dasgupta, and L. R. Gasques, Phys. Rev. Lett. **98**, 152701 (2007); arXiv:**nucl-th/0703041**(2007).
24. Y. Tokimoto *et al.*, Phys. Rev. C **63**, 035801 (2001).
25. M. M. de Moura *et al.*, Nucl. Instr. Meth. A **471**, 368 (2001).
26. G. G. Ohlsen, Nucl. Instr. Meth. **37**, 240 (1965).
27. D. Scholz *et al.*, Nucl. Phys. A **288**, 351 (1977).
28. J. E. Mason *et al.*, Phys. Rev. C **45**, 2870 (1992).
29. R. Kanungo *et al.*, Nucl. Phys. A **599**, 579 (1996).
30. K. Alder *et al.*, Rev. Mod. Phys. **28**, 432 (1956).
31. D.R. Tilley *et al.*, Nucl. Phys. A **708**, 3 (2002).